Influence of Solute−Solvent Hydrogen Bonding on Intramolecular Magnetic Exchange Interaction in Aminoxyl Diradicals: A QM/MM Broken-Symmetry DFT Study

Md. Ehesan Ali,*,† Peter M. Oppeneer,† and Sambhu N. Datta‡

Department of Physics and Materials Science, Uppsala University, Box 530, SE-75121 Uppsala, Sweden, and Department of Chemistry, Indian Institute of Technology-Bombay, Powai, Mumbai 400076, India

Received: October 6, 2008

We have investigated the effect of nitroxide radical−water hydrogen bonding ($NO^{\bullet}\cdots H_2O$) on the intramolecular magnetic exchange interaction (J) for biologically relevant aminoxyl diradicals. We adopt a combination of broken-symmetry density functional theory and the quantum mechanics/molecular mechanics (QM/MM) approach. We find that the presence of hydrogen bonding reorients the radical spin density on $-NO^{\bullet}$. This phenomenon reduces the effective distance between the two interacting localized spin centers that eventually increases the intramolecular magnetic exchange interaction. We have also investigated the functional variation of the magnetic exchange interaction, using various GGA (BLYP, PBE, HCTH407), meta-GGA (TPSS, VXSC), and hybrid (O3LYP, B3LYP, B3P86, B3PW91, and PBE0) functionals.

I. Introduction

In organic molecular magnetic materials, stable radicals act as the essential building blocks. The spin−spin couplings in the radicals are responsible for the magnetic properties of these organic systems. Moreover, the diradicals with ground-state spin $S = 1$ have attracted scientific attention even beyond organic molecular magnetism, for example, in biomedical applications.[1,2]

Aminoxyl radicals are known to be the counter agents for magnetic resonance imaging (MRI).[3] Presently, the dominant contrast agents for magnetic resonance imaging (MRI) are Gd ($S = {}^7/_2$) and other paramagnetic metal ions. However, in conjunction with the favorable *in vivo* properties of aminoxyls with $S > {}^1/_2$ at room temperature, these diradicals provide a novel organic contrast agent for MRI. Importantly, the potential biological applications of these radicals require solubility in water. Numerous attempts are reported in the literature to increase the water solubility of aminoxyl radicals.[4] Rajca et al. have synthesized various aminoxyl radicals with the triplet ground state.[5,6] It is well-known that the molecular topology, aromaticity of the coupler, and presence of electron donating and withdrawing groups in the exchange pathway can greatly affect the magnetic exchange interactions.[7−9]

Here, we focus on the change of magnetic properties due to the solvation of radical systems. In this work, the impact of solvation on the magnetic properties is established to be twofold. One is topological reorientation of radical systems in the presence of the solvent. The other is the solute−solvent chemical interaction. To account for the solvation effects, we use explicit static solvation models, with up to 60 H_2O molecules in the calculations of magnetic properties of radicals.

II. Computational Methodology

The calculation of magnetic exchange interactions is a challenging task due to the multideterminant nature of the associated wave function. The multiconfigurational CI approach is a logical solution, but it is impractical due to computational complexity for larger systems as far as time and resources are concerned. The broken-symmetry (BS) method as proposed by Noodleman and co-workers provided the best solutions so far.[10] A large amount of literature can be found concerning the theoretical formulations, successes, failures, and improvements of the broken-symmetry methodology.[11−16]

We performed quantum mechanics/molecular mechanics (QM/MM) calculations for the explicit treatment of the solvation effect in combination with the broken-symmetry approach. We used the hybrid method ONIOM for two-layer QM/MM calculations.[17] All of the geometry optimizations were performed using unrestricted hybrid density functional theory with Becke's three-parameter exchange functional[18] and the nonlocal Lee−Yang−Parr correlation functional[19] (UB3LYP model). The hybrid functional includes a mixture of 20% Hartree−Fock (HF) exchange with the nonlocal/gradient-corrected exchange-correlation functional. The basis set used for this purpose is 6-311+G(d,p). For ONIOM optimizations, the higher level (QM region) was treated with the above-mentioned method only, whereas the lower level was treated with the universal force field (UFF). All of the magnetic exchange interactions (J) were calculated using the Ginsberg−Noodleman−Davidson spin projected formula, $J = (E_{BS} - E_T)/S_{max}^2$, because the overlap integral S_{ab} was very small and the spin contamination in the BS solution was negligibly low. The quantum chemical code Gaussian 03 was used for this work.[20]

III. Results and Discussion

The molecular geometries for triplet states in the single molecule environments were optimized with the UB3LYP method using the 6-311+G(d,p) basis sets. The magnetic exchange coupling constants were calculated using the UB3LYP/6-311G(d,p) level. The systems under investigation in this work, **1**−**4**, are shown in Figure 1. Rajca et al. synthesized these diradicals and studied the magnetic properties in solutions. They also reported the solid-state magnetic exchange interaction as well for **2**−**4**. The observed J value for **1** in solution is 225 cm^{-1}.[5] The reported lower limits of J values for **2**−**3** in solution are 70 cm^{-1} and in solid state 104 cm^{-1}. The lower limit of J

* To whom correspondence should be addressed. Email: ehesan.ali@fysik.uu.se.
† Uppsala University.
‡ Indian Institute of Technology-Bombay.

10.1021/jp901922j CCC: $40.75
Published on Web 03/30/2009

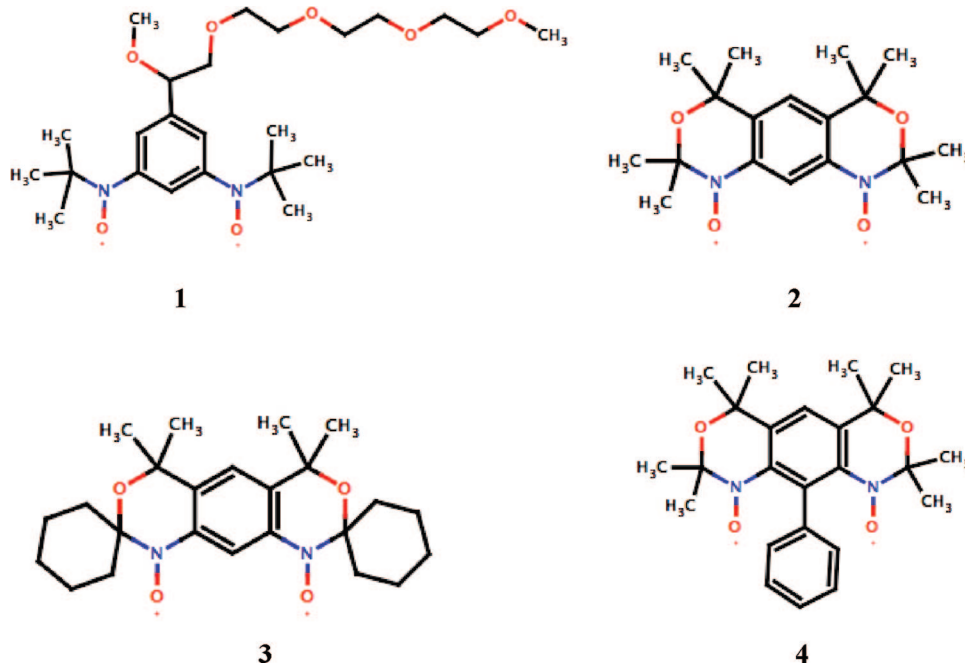

Figure 1. Schematic diagram of the aminoxyl diradicals, labeled **1**−**4**, that are investigated in this work. The NO• is the radical species for all of the cases.

TABLE 1: Intramolecular Magnetic Coupling Constant *J* (in cm^{-1}) Varying the Exchange-Correlation Functional Using Single Molecule Optimized Geometry

	J (cm^{-1})				
functional	**1**	**1′** [a]	**2**	**3**	**4**
			GGA		
BLYP	75.76	110.49	330.32	312.29	272.39
PBE	85.25	138.72	364.78	346.11	293.53
HCTH407	92.34	184.04	422.17	398.89	325.16
			meta-GGA		
TPSS	102.21	220.79	469.15	446.27	344.55
VSXC	103.35	212.88	494.58	470.52	377.98
			Hybrid		
O3LYP	95.05	244.14	484.44	460.89	340.80
B3LYP	104.08	282.73	547.23	521.66	372.01
B3P86	114.34	314.04	589.85	563.01	399.04
B3PW91	116.76	322.80	601.87	574.71	405.86
PBE0	125.22	360.96	632.12	632.12	438.20
Exp.		225.6[b]	>70[b]	>70[b]	>70[b]
			>104.3[c]	>104.3[c]	∼139−278[c]

[a] The conformational isomer **1′** of **1**, where the dihedral angles C−C−N−O are rotated from 41 to 0°, which makes −NO isoplanar with the *m*-phenyl plane. [b] In solution. [c] In solid state.

TABLE 2: Calculated *J* Values (in cm^{-1}) Obtained with Broken-Symmetry (BS) Methods in the QM Level [UB3LYP/6-311G(d,p)] for ONIOM as Well as in Single Molecules

functional and methods of *J* calculation	geometry used	**1**	**2**	**3**	**4**
		O3LYP			
ONIOM-BS[a]	ONIOM including few H_2O in QM region	71.14	503.52	478.27	354.10
BS[b]	above geometry with no solvent	68.58	474.55	465.64	303.18
		B3LYP			
ONIOM-BS[a]	ONIOM including H_2O in QM region	79.71	586.70	526.95	399.39
BS[b]	above geometry with no solvent	73.56	568.35	524.80	329.97

[a] ONIOM-BS refers to BS-DFT calculation in the QM sphere of a ONIOM calculation. [b] BS refers to the traditional BS-DFT calculations, as mentioned in refs 8 and 10−16.

for diradical **4** in solution is 70 cm^{-1} and in solid state in the range ∼139−278 cm^{-1}.[6]

The calculated *J* value for **1** in UB3LYP yielded only 104 cm^{-1}, which differs markedly from the observed value. This

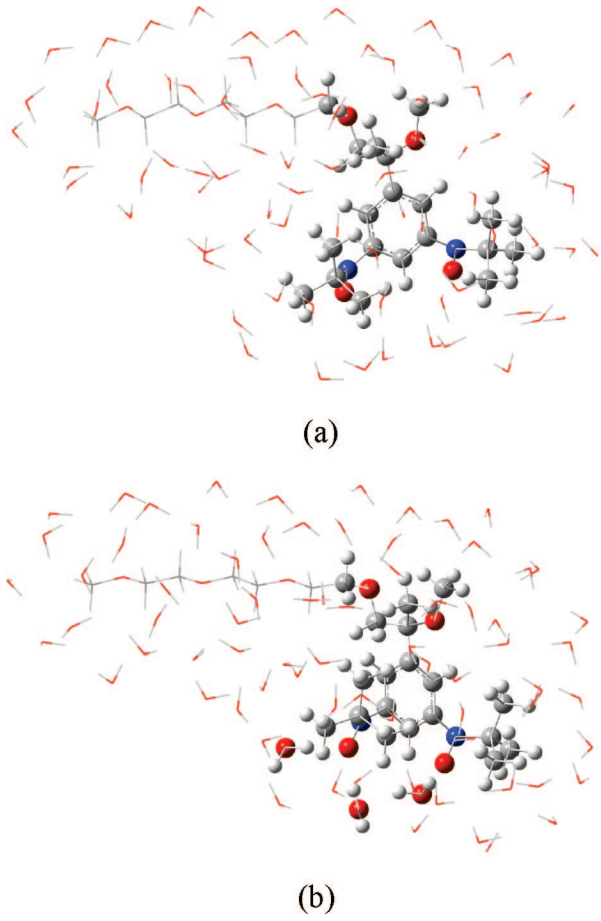

Figure 2. Solvated ONIOM optimized diradical **1**. The ball-and-stick model shows the QM region, whereas the sticks only show the MM region: (a) first ONIOM optimized geometry where H_2O molecules are apart from the $-NO^{\bullet}$ group by ~3.5 Å; (b) second ONIOM optimized geometry (few water molecules are included in QM spheres) where H_2O's are ~2.0 Å away from the $-NO^{\bullet}$ group.

disagreement could be a shortcoming of the choice of exchange-correlation functional, because the calculated J values were found to be a functional dependent quantity.[21] The magnetic coupling is strongly dominated by the electron exchange and correlation functional. It has also been observed that both dynamical and nondynamical correlation contributions are necessary to be included in the calculation of the magnetic exchange interaction.[22] Thus, the choice of exchange-correlation functional should be such that one can obtain a good match between the theoretical and experimental magnetic exchange interactions. We have systematically calculated the magnetic exchange coupling constants varying the exchange-correlation functional.

Truhlar et al. have recently proposed hybrid and nonhybrid meta-GGA functionals known as the M0X family that are very successful in reproducing many important molecular properties.[23] Valero et al. and Ruiz et al. have independently investigated the magnetic exchange coupling constant using the M0X functional.[24,25] They observed the equal success of hybrid-M0X with the PBE0 and B3LYP functionals.

In this work, we have chosen generalized gradient approximate (GGA) functionals (BLYP, PBE, HCTH07), kinetic energy density (τ) dependent functionals know as meta-GGA (TPSS, VXSC), Handy's three-parameter hybrid functional (O3LYP), Becke's three-parameter hybrid functionals (B3LYP, B3P86, B3PW91), and the parameter free hybrid functional (PBE0).[26] The calculated magnetic exchange interactions are given in Table 1. However, for **1**, we find that the larger deviation of J from the observed value is due to the large out-of-plane rotation of $-NO^{\bullet}$ from the plane of the coupler. The geometry optimization was not able to produce the proper planar structure in single molecule as well as in ONIOM optimization due to the highly flexible unrestricted conformational nature of phenyl$-NO^{\bullet}$ bonds in **1**. The absence of exact local solvent environment in the computation even in the ONIOM calculation is the other possible reason. We speculate that the extensive *ab initio* molecular dynamics (AIMD) calculations would be able to resolve the proper solvated structure, but this is beyond the scope of the present interest. Here, we have manually rotated the NO plane to make it coplanar with the *m*-phenyl coupler's plane. The rest of the optimized geometry of species **1** is kept intact. This new conformational isomer is labeled as **1′**, and the results are given in Table 1. However, for **2**−**4**, due to close structures, there is no possibility of such conformational isomers.

In our calculations, we observed that the local GGA functional underestimates the J values for these species with the triplet ground state. The nonhybrid kinetic energy density dependent gradient-corrected functional of Tao, Perdew, Staroverov, and Scuseria (TPSS) and the von Voorhis−Scuseria (VSXC) functional provide an intermediate and comparable J value for **1** and **4**, but for **4**, GGA gives slightly better results in comparison to the experimentally reported values. For **2** and **3,** a direct comparison is not possible, as the exact J value is not reported. Ciofini, Illas, and Adamo have also observed the success of the meta-GGA functional in producing the magnetic exchange interactions of solids.[27]

Inclusion of the exact exchange into the GGA functional caused the J value to increase systematically. The contributions of the nonlocal Hartree−Fock exchange in all of the hybrid functionals considered in this work are 11.61% in O3LYP, 20% in B3LYP, B3PB86, and B3PW91, and 25% in PBE0, respectively. The contribution of the nonlocal correlation functional is also significant along with that of the exact exchange functional. PBE0 here overestimates the J values. The hybrid functional with compact exchange functional OPTX (modified B88X) along with 11.61% HF and LYP correlations functional (i.e., O3LYP) produces a good match of the calculated magnetic exchange interactions along with the reported J values for molecule **1** (Table 2).

Solvation Effect. To include the solvent effects explicitly on the molecular geometries, QM/MM calculations were performed. In this case, the optimizations were performed,

TABLE 3: Average Mulliken Spin Density on the Nitrogen (N) and Oxygen (O) of $-NO^{\bullet}$ Radical Subunits Obtained in the Magnetic Ground State

	1		**2**		**3**		**4**	
molecule	N	O	N	O	N	O	N	O
single molecule	0.40	0.52	0.34	0.49	0.35	0.48	0.35	0.52
first ONIOM optimized molecules	0.40	0.53	0.34	0.49	0.35	0.48	0.35	0.51
second ONIOM including closest H_2O in QM region	0.45	0.47	0.39	0.42	0.40	0.40	0.43	0.41
above geometry with no solvent	0.40	0.53	0.34	0.49	0.35	0.48	0.35	0.52

treating the radical system at a higher level and water (solvent) molecules in the lower level. For the higher level (the QM region), we used the UB3LYP/6-311+G(d,p) methodology and the MM portions were treated with the universal force field (UFF). All of the previously optimized single molecules are reoptimized using this ONIOM technique. The optimized geometry for molecule **1** along with the considered solvent molecules (water) is shown in Figure 2a.

To understand this phenomenon, we further analyzed the Mulliken spin density for the free molecule, for the first ONIOM optimized molecule ($NO^{\bullet}\cdots H_2O$ distances are ~3.5 Å), and for the second ONIOM optimized molecule ($NO^{\bullet}\cdots H_2O$ distances are ~2.0 Å). The spin densities of the radical centers are effectively localized within the N−O region and display a larger localization on the radical oxygen atoms (Table 3). This remains valid for the single molecules, and for the first ONIOM optimized geometries where there is no effective hydrogen bond. However, upon inclusion of hydrogen bonding with improved models, we notice a rearrangement of the spin density of the −NO.

The formation of a hydrogen bond shifts the spin density from the oxygen to nitrogen atoms. This reorientation of the spin density reduces the effective distance between the two interacting radical centers. As a result, *the strength of the intramolecular magnetic exchange interaction increases*.

IV. Conclusions

We have calculated the magnetic exchange interaction of four recently synthesized and biologically important aminoxyl radicals with different GGA, meta-GGA, and hybrid functionals. All of those radical species are ferromagnetically coupled. We find that meta-GGA and O3LYP functionals produce comparable results, but a direct comparison with the experimental results is not possible in the present cases, as the *J* values are experimentally not sharply defined except for diradical **1**. We also find that the solute−solvent chemical interaction strongly influences the intramolecular magnetic exchange interaction. The formation of a $NO^{\bullet}\cdots H_2O$ hydrogen bond in solution increases the electron density on the N atoms. This phenomenon of reorientation of the spin density increases the magnetic exchange interaction in the solution due to the shorter interaction between the two localized spin centers in the diradicals.

Acknowledgment. The computational facility at the Swedish National Infrastructure for Computing (SNIC) is gratefully acknowledged. M.E.A. and P.M.O. acknowledge support from the Carl Tryggers Foundation. S.N.D. acknowledges support from the Council of Scientific and Industrial Research (CSIR).

References and Notes

(1) (a) Tamura, M.; Nakazawa, Y.; Shiomi, D.; Nozawa, K.; Hosokoshi, Y.; Ishikawa, M.; Takahashi, M.; Kinoshita, M. *Chem. Phys. Lett.* **1991**, *186*, 401. (b) Nakazawa, Y.; Tamura, M.; Shirakawa, N.; Shiomi, D.; Takahashi, M.; Kinoshita, M.; Ishikawa, M. *Phys. Rev. B* **1992**, *46*, 8906. (c) *Molecular Magnetism, New Magnetic Materials*; Itoh, K., Kinoshita, M., Eds.; Gordon and Breach: Amsterdam, The Netherlands, 2000. (d) Rajca, A. *Chem. Rev.* **1994**, *94*, 871.

(2) Matsumoto, K.; Hyodo, F.; Matsumoto, A.; Koretsky, A. P.; Sowers, A. L.; Mitchell, J. B.; Krishna, M. C. *Clin. Cancer Res.* **2006**, *12*, 2455.

(3) Sosnovsky, G.; Rao, N. U. M.; Li, S. W.; Swartz, H. M. *J. Org. Chem.* **1989**, *54*, 3667.

(4) (a) Marx, L.; Rassat, A. *Chem. Commun.* **2002**, 632. (b) Huang, W.; Charleux, B.; Chiarelli, R.; Marx, L.; Rassat, A.; Vairon, J.-P. *Macromol. Chem. Phys.* **2002**, *203*, 1715.

(5) Spagnol, G.; Shiraishi, K.; Rajca, S.; Rajca, A. *Chem. Commun.* **2005**, 5047.

(6) Rajca, A.; Takahashi, M.; Pink, M.; Spagnol, G.; Rajca, S. *J. Am. Chem. Soc.* **2007**, *129*, 10159.

(7) Barone, V.; Bencini, A.; Matteo, A. *J. Am. Chem. Soc.* **1997**, *119*, 10831.

(8) Ali, Md. E.; Datta, S. N. *J. Phys. Chem. A* **2006**, *110*, 2776.

(9) Lahti, P. M. *Magnetic Properties of Organic Materials*; CRC Press: 1999.

(10) Noodleman, L.; Davidson, E. R. *Chem. Phys.* **1986**, *109*, 131.

(11) Bencini, A.; Totti, F.; Daul, C. A.; Doclo, K.; Fantucci, P.; Barone, V. *Inorg. Chem.* **1997**, *36*, 5022.

(12) Ruiz, E.; Cano, J.; Alvarez, S.; Alemany, P. *J. Comput. Chem.* **1999**, *20*, 1391.

(13) (a) Martin, R. L.; Illas, F. *Phys. Rev. Lett.* **1997**, *79*, 1539. (b) de Moreira, P. R. I.; Illas, F. *Phys. Chem. Chem. Phys.* **2006**, *8*, 1645.

(14) Yamaguchi, K.; Jensen, F.; Dorigo, A.; Houk, K. N. *Chem. Phys. Lett.* **1988**, *149*, 537.

(15) (a) Schreiner, E.; Nair, N. N.; Pollet, R.; Staemmler, V.; Marx, D. *Proc. Natl. Acad. Sci. U.S.A.* **2007**, *104*, 20725. (b) Nair, N. N.; Schreiner, E.; Pollet, R.; Staemmler, V.; Marx, D. *J. Chem. Theory Comput.* **2008**, *4*, 1174.

(16) Bencini, A.; Totti, F. *J. Chem. Theory Comput.* **2009**, *5*, 144.

(17) (a) Svensson, M.; Humbel, S.; Froese, R. D. J.; Mastubara, T.; Sieber, S.; Morokuma, K. *J. Phys. Chem.* **1996**, *100*, 19357. (b) Dapprich, S.; Komaromi, I.; Byun, K. S.; Morokuma, K.; Frisch, M. J. *THEOCHEM* **1999**, *461−462*, 1.

(18) Becke, A. D. *Phys. Rev. A* **1988**, *38*, 3098.

(19) Lee, C.; Yang, W.; Parr, R. G. *Phys. Rev. B* **1998**, *37*, 785.

(20) Frisch, M. J.; Trucks, G. W.; Schlegel, H. B.; Scuseria, G. E.; Robb, M. A.; Cheeseman, J. R.; Montgomery, J. A., Jr.; Vreven, T.; Kudin, K. N.; Burant, J. C.; Millam, J. M.; Iyengar, S. S.; Tomasi, J.; Barone, V.; Mennucci, B.; Cossi, M.; Scalmani, G.; Rega, N.; Petersson, G. A.; Nakatsuji, H.; Hada, M.; Ehara, M.; Toyota, K.; Fukuda, R.; Hasegawa, J.; Ishida, M.; Nakajima, T.; Honda, Y.; Kitao, O.; Nakai, H.; Klene, M.; Li, X.; Knox, J. E.; Hratchian, H. P.; Cross, J. B.; Bakken, V.; Adamo, C.; Jaramillo, J.; Gomperts, R.; Stratmann, R. E.; Yazyev, O.; Austin, A. J.; Cammi, R.; Pomelli, C.; Ochterski, J. W.; Ayala, P. Y.; Morokuma, K.; Voth, G. A.; Salvador, P.; Dannenberg, J. J.; Zakrzewski, V. G.; Dapprich, S.; Daniels, A. D.; Strain, M. C.; Farkas, O.; Malick, D. K.; Rabuck, A. D.; Raghavachari, K.; Foresman, J. B.; Ortiz, J. V.; Cui, Q.; Baboul, A. G.; Clifford, S.; Cioslowski, J.; Stefanov, B. B.; Liu, G.; Liashenko, A.; Piskorz, P.; Komaromi, I.; Martin, R. L.; Fox, D. J.; Keith, T.; Al-Laham, M. A.; Peng, C. Y.; Nanayakkara, A.; Challacombe, M.; Gill, P. M. W.; Johnson, B.; Chen, W.; Wong, M. W.; Gonzalez, C.; Pople, J. A. *Gaussian 03*, revision C.02; Gaussian, Inc.: Wallingford CT, 2004.

(21) (a) de Moreira, P. R. I.; Costa, R.; Filatov, M.; Illas, F. *J. Chem. Theory Comput.* **2007**, *3*, 764. (b) Ruiz, E.; Rodríguez-Fortea, A.; Tercero, J.; Cauchy, T.; Massobrio, C. *J. Chem. Phys.* **2005**, *123*, 074102. (c) Mitani, M.; Yamaki, D.; Takano, Y.; Kitagawa, Y.; Yoshioka, Y.; Yamaguchi, K. *J. Chem. Phys.* **2000**, *113*, 10486.

(22) (a) Bofill, J. M.; Pulay, P. *J. Chem. Phys.* **1989**, *90*, 3637. (b) Illas, F.; de Moreira, P. R. I.; Bofill, J. M.; Filatov, M. *Phys. Rev. B* **2004**, *70*, 132414.

(23) (a) Zhao, Y.; Truhlar, D. G. *J. Chem. Phys.* **2006**, *125*, 194101. (b) Marenich, A. V.; Olson, R. M.; Kelly, C. P.; Cramer, C. J.; Truhlar, D. G. *J. Chem. Theory Comput.* **2007**, *3*, 2011.

(24) Valero, R.; Costa, R.; de Moreira, P. R. I.; Truhlar, D. G.; Illas, F. *J. Chem. Phys.* **2008**, *128*, 114103.

(25) Ruiz, E. *Chem. Phys. Lett.* **2008**, *460*, 336.

(26) (a) Perdew, J. P.; Burke, K.; Ernzerhof, M. *Phys. Rev. Lett.* **1997**, *78*, 1396. (b) Perdew, J. P.; Burke, K.; Ernzerhof, M. *Phys. Rev. Lett.* **1996**, *77*, 3865. (c) Handy, N. C.; Cohen, A. J. *Mol. Phys.* **2001**, *99*, 403. (d) Tao, J. M.; Perdew, J. P.; Staroverov, V. N.; Scuseria, G. E. *Phys. Rev. Lett.* **2003**, *91*, 146401. (e) Van Voorhis, T.; Scuseria, G. E. *J. Chem. Phys.* **1998**, *109*, 400. (f) Hamprecht, F. A.; Cohen, A. J.; Tozer, D. J.; Handy, N. C. *J. Chem. Phys.* **1998**, *109*, 6264.

(27) Ciofini, I.; Illas, F.; Adamo, C. *J. Chem. Phys.* **2004**, *120*, 3811.

JP901922J